



Contents lists available at ScienceDirect

European Journal of Pharmaceutical Sciences

journal homepage: [www.elsevier.com/locate/ejps](http://www.elsevier.com/locate/ejps)

# Investigation of recrystallization of amorphous trehalose through hot-humidity stage X-ray powder diffraction

Orsolya Jójárt-Laczkovich<sup>a,\*</sup>, Gábor Katona<sup>a,b</sup>, Zoltán Aigner<sup>a</sup>, Piroska Szabó-Révész<sup>a</sup>

<sup>a</sup> Department of Pharmaceutical Technology, University of Szeged, Szeged, Hungary

<sup>b</sup> Richter Gedeon Plc., Gyömrői 19-21, H-1103 Budapest, Hungary

## ARTICLE INFO

### Article history:

Received 11 February 2016

Received in revised form 25 July 2016

Accepted 2 August 2016

Available online xxxx

### Keywords:

Trehalose

Recrystallization

Activation energy

Hot-humidity stage XRPD

DSC

## ABSTRACT

The aim of this work was an investigation of the physical changes of the amorphous model material spray-dried trehalose through the use of various analytical techniques and to identify a suitable, rapid method able to quantify the changes. The crystallinity changes and recrystallization process of amorphous samples were investigated by hot-humidity stage X-ray powder diffractometry (HH-XRPD) with fresh samples, conventional X-ray powder diffractometry (XRPD) used stored samples and by differential scanning calorimetry (DSC). The data from the three methods were compared and the various forms of trehalose were analysed. HH-XRPD demonstrated that the recrystallization began at 40 and 60 °C up to 45% RH and at 70 °C up to 30% RH into dihydrate form. At 70 °C up to 60% RH the anhydrous form of trehalose appeared too. Conventional XRPD results showed, that in the 28 days stored samples the dihydrate form was detected at 40 °C, 50% RH. Storage at 60 °C, 40% RH resulted in the appearance of the anhydrous form and at 60 °C, 50% RH both polymorphic forms were detected. By carrying out the DSC measurements at different temperatures the fraction of recrystallized trehalose dihydrate was detected. The recrystallization investigated by HH-XRPD and DSC followed Avrami kinetics, the calculated rate constants of isothermal crystallization ( $K$ ) were same. Both HH-XRPD and conventional XRPD was suitable for the detection of the physical changes of the amorphous model material. DSC measurements showed similar results as HH-XRPD. Primarily HH-XRPD could be suggested for prediction, because the method is fast and every changes could be studied on one sample.

© 2016 Elsevier B.V. All rights reserved.

## 1. Introduction

Trehalose is a natural sugar, but it is also synthesized and produced on a large scale industrially. It is widely applied in the cosmetic, agricultural, food and drug industries. In drug formulations, it is utilized as an active pharmaceutical ingredient or as a technological auxiliary agent. Trehalose could be also an active agent as chemical chaperone which is used to treat Creutzfeldt-Jakob disease, cystic fibrosis and amyloid disorders that prevent protein aggregation (Aguib et al., 2009). In oral medication, it displays antidepressant properties in the mouse model of depression, possibly through reducing the p62/Beclin-1 ratio and increasing autophagy in the frontal cortex (Kara et al., 2013).

The most important applications of trehalose as a pharmaceutical excipient are to preserve enzymes, to stabilize vaccines at room temperature for storage, and to protect mammalian cells from damage during lyophilization. Trehalose concentrates the water near the protein, and it can be transformed to its native structure after lyophilization and regain its function (Timasheff, 2002). The protein-stabilizing ability of

trehalose is utilized in many areas of industry, e.g. as a moisturizer or to stabilize liposomes (Tanaka et al., 1992). As an auxiliary component, it is often applied as a carrier of dry powder inhalation (DPI) systems. For this purpose,  $\alpha$ -lactose monohydrate is normally used, but lactose may react with the amino group, so proteins and peptides cannot be formulated with it. In this case, lactose must be substituted with trehalose, raffinose or sucrose. These non-reducing sugars have the common advantage of protecting proteins or peptides against different stress conditions during spray-drying. They substitute the hydrogen-bonds in water, and form viscous mixtures with proteins, resulting in products with high glass temperatures of the product (Maas et al., 2011).

Trehalose is often produced as an excipient by spray-drying (Ógáin et al., 2011; Islam and Gladki, 2008; Gradon and Sosnowski, 2014; Pomázi et al., 2011; Maurya et al., 2005a; Maurya et al., 2005b; Moran and Buckton, 2007a; Amaro et al., 2015), freeze-drying (Murugappan et al., 2013; Nakamura et al., 2008; Crowe et al., 2003; Jovanovic et al., 2006; Claus et al., 2011) and spray-freeze-drying (Tonniss et al., 2014; Yu et al., 2006) in pharmaceutical technology. Trehalose tends to undergo amorphization, and the amorphous form is readily prepared by using a solvent method such as spray- or freeze-drying. The recrystallization kinetics can be followed which is important because of the appearance of polymorph forms (Sussich and Cesáro, 2008). Trehalose has 4

\* Corresponding author at: Department of Pharmaceutical Technology, University of Szeged, H-6720 Szeged, Eötvös u. 6, Hungary.

E-mail address: [laczkovo@pharm.u-szeged.hu](mailto:laczkovo@pharm.u-szeged.hu) (O. Jójárt-Laczkovich).

**Table 1**  
Melting points of trehalose polymorphs (Sussich and Cesáro, 2008).

Polymorph	Melting point (°C)
Trehalose- $\alpha$ (anhydrous)	120
Trehalose- $\beta$ (anhydrous)	215
Trehalose- $\gamma$ (anhydrous)	118–122
Trehalose-h (dihydrate)	100–110

polymorphic forms (Table 1). This is especially important in the case of DPI because of the preparation methods and the storage conditions of the product. In this work one of the most efficient amorphization technology, spray-drying was selected for preparing amorphous trehalose. This method results in a monodisperse product with suitable particle size and excellent flowability.

Various analytical methods are available to investigate amorphization (Jójárt-Laczovich and Szabó-Révész, 2010; Jójárt-Laczovich and Szabó-Révész, 2011; Danciu et al., 2014; Jug and Bećirević-Lačan, 2004), recrystallization, polymorphic conversions, and the dehydration and rehydration mechanisms of different materials (Szakonyi and Zelkó, 2012). Common techniques are differential scanning calorimetry (DSC) and X-ray powder diffraction (XRPD) measurements. Besides these possibilities, dynamic vapour sorption (Jones et al., 2006), Karl Fischer moisture titration, isothermal thermogravimetric analysis (Taylor and York, 1998) and simultaneous techniques (DSC-XRPD and TG-DTA) have also been described in the case of trehalose (Furuki et al., 2005; Mah et al., 2015). A modern investigation method is hot-humidity stage X-ray powder diffraction (HH-XRPD), whereby temperature and RH are variable. Through HH-XRPD analysis, complex pharmaceutical solid-state reactions, including crystal structure transformations, can be in situ characterized and followed. This method rapidly provides information about polymorph conversions and recrystallization kinetics, and short-term stability testing can be carried out during preformulation studies. Examples of the polymorphic transformation of some active and auxiliary agents (naloxone, naltrexone and aspartame) are to be found in the literature (Guguta et al., 2009; Guguta et al., 2008).

The focus of this work was an investigation of the recrystallization process of the amorphous model material spray-dried trehalose and to find a suitable method to predict the recrystallization of amorphous sample during a preformulation study. In a comparison study three, different methods (HH-XRPD, XRPD, DSC) were used to analyse the crystallinity changes.

## 2. Materials and methods

### 2.1. Materials

D-(+)-trehalose dihydrate h-form was purchased from Karl Roth GmbH + Co. KG. (Karlsruhe, Germany). This was regarded as 100% crystalline material. The water content was  $9.5 \pm 0.5\%$  and the sulphate content was  $<0.5\%$ . Its specific rotation was  $178 \pm 2^\circ$ .

Anhydrous D-(+)-trehalose  $\beta$ -form was produced by dehydration of trehalose dihydrate at  $85^\circ\text{C}$  during 4 h under vacuum (Nagase et al., 2002) and checked the within 24 h both with DSC and XRPD.

**Table 2**  
Operation parameters for the preparation of spray-dried trehalose.

Operating parameters	Settings
Inlet temperature (°C)	130–140
Outlet temperature (°C)	75–92
Feed rate (ml/min)	2
Pressure (bar)	4.8
Atomizer flow rate (normolitre/h)	600
Aspirator (%)	80

**Table 3**  
Different storage conditions of amorphous samples.

Temperature (°C)	Relative humidity (%)	Storage time (day)
$25 \pm 2$	$32 \pm 5$	1
$40 \pm 2$	$30 \pm 5$	28
	$40 \pm 5$	28
	$50 \pm 5$	28
$60 \pm 2$	$30 \pm 5$	28
	$40 \pm 5$	28
	$50 \pm 5$	28

### 2.2. Preparation of spray-dried trehalose

Trehalose dihydrate was spray-dried from 10% solutions in water (5 g of trehalose and 45 g of water), using a Büchi 191 Mini Spray Dryer (Büchi, Switzerland). The parameters used are given in Table 2 (Moran and Buckton, 2007b). The spray-dried products were stored in a desiccator over cobalt(II) chloride-contaminated silicon dioxide ( $25 \pm 2^\circ\text{C}$ ,  $32 \pm 5\%$  RH) until use and were X-ray amorphous.

### 2.3. Preparation of physical mixtures

Physical mixtures of spray-dried (amorphous) and the two different crystalline form of trehalose were prepared to achieve 0, 5, 10, 30, 50, 70, 90, 95 and 100% crystalline content by mass. The components were weighed to a total amount of 0.50 g and were mixed homogenous in a trituration mortar.

### 2.4. HH-XRPD

HH-XRPD analysis was performed on the spray-dried amorphous samples within 24 h by using a Bruker D8 Advance X-ray Diffractometer (Bruker AXS GmbH, Karlsruhe, Germany) with Cu K $\alpha$  radiation ( $\lambda = 1.5406 \text{ \AA}$ ) installed with an MRI Basic hot-humidity stage and a VANTEC-1 detector. The samples were scanned at 40 kV and 40 mA. The angular range was from  $3^\circ$  to  $40^\circ 2\theta$ , at a step time of 0.1 s and a step size of  $0.007^\circ$ . An ANS-Sycoshot humidity control device was coupled to the XRPD, which injected humidity into a controlled dry gas flow. The carrier gas was compressed air with a 0.5 l/min flow. The sample was taken in a Ni-coated sample holder. The RH was set at 10, 20, 30, 40, 45, 50, 60 and 70% at  $40^\circ\text{C}$ ,  $60^\circ\text{C}$  and  $70^\circ\text{C}$  controlled temperatures, and the samples were kept in each condition for 1 h before measurement. All manipulations, K $\alpha$  2-stripping, background removal and signal to noise smoothing of the area under the peaks of diffractograms were performed with DIFFRACTPLUS EVA software.

### 2.5. XRPD

XRPD analysis was performed with a Bruker D8 Advance diffractometer (Bruker AXS GmbH, Karlsruhe, Germany) with Cu K $\alpha$  radiation ( $\lambda = 1.5406 \text{ \AA}$ ) and a VANTEC-1 detector. Both the physical mixtures and the stored amorphous samples were scanned at 40 kV and 40 mA. The angular range was  $3^\circ$  to  $40^\circ 2\theta$ , at a step time of 0.1 s and a step size of  $0.007^\circ$ . The sample was placed on a quartz holder, measured at ambient temperature and RH. All manipulations, K $\alpha$  2-stripping, background removal and smoothing of the area under the peaks of diffractograms were performed with DIFFRACTPLUS EVA software. The determination of the polymorph form was based on the Cambridge Crystallographic Data Centre (CCDC ID: Al631510) X-ray powder diffractograms.

### 2.6. Storage conditions

One part of the spray-dried product was stored in a desiccator over cobalt(II) chloride-contaminated silicon dioxide ( $25 \pm 2^\circ\text{C}$ ,  $32 \pm 5\%$

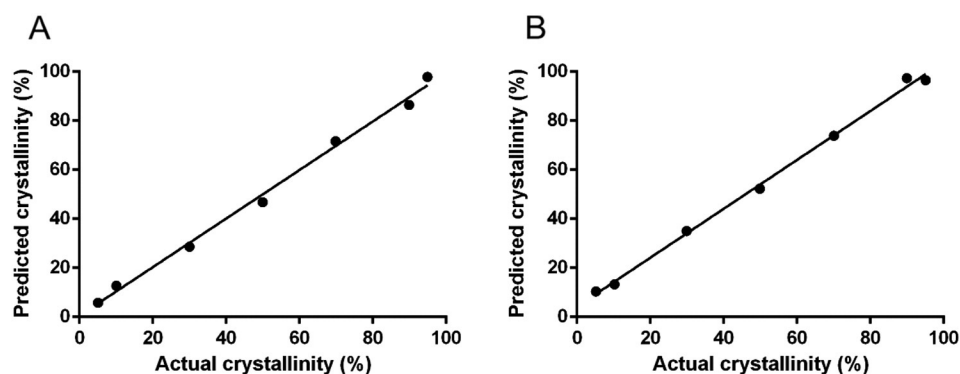


**Fig. 1.** Relation between predicted and actual crystallinity of physical mixtures of crystalline trehalose dihydrate - amorphous form (A), anhydrous trehalose - amorphous form (B) determined by conventional X-ray powder diffraction.

RH) until HH-XRPD measurements. The remainder was divided into 6 parts and stored for 28 days at 40 °C and 60 °C, in 3–3 hygostats, where the RH was set to 30%, 40% and 50% RH. In each dessicator and hygostates, there was a digital humidity meter during the storage for controlling the relative humidity. These samples were investigated with XRPD (Table 3).

### 2.7. Calculation of the recrystallization kinetics

The recrystallization kinetics was modelled by using the Avrami equation (Eq. (1)):

$$1 - \alpha = \exp(-Kt^n) \quad (1)$$

where  $\alpha$  is the fraction of recrystallized trehalose at time  $t$ ,  $K$  is the rate constant and  $n$  is the Avrami index, a parameter characteristic of the nucleation and growth mechanism of crystals.

The fraction of recrystallized trehalose ( $\alpha$ ) was calculated from the area under the characteristic peaks using the following equation (Eq. (2)):

$$\alpha = \frac{A_{\text{crystalline}}}{A_{\text{crystalline}} + A_{\text{amorphous}}} * 100 \quad (2)$$

where  $\alpha$  is the crystalline fraction,  $A$  is the area of characteristic crystalline peaks and amorphous sign. Three characteristic peaks each were selected from the diffractograms of trehalose dihydrate (at 8.531°, 12.552° and 14.224° 2 $\theta$ ) and anhydrous trehalose (at 6.572°, 20.351° and 24.792° 2 $\theta$ ). The XRPD instrument was calibrated every day with corundum during the 28 days measurement to minimize the day to day intensity changes in XRPD emission.

**Table 4**

The degree of crystallinity calculated from the HH-XRPD data (A: amorphous, h-form: dihydrate,  $\beta$ -form: anhydrous).

Time [min, RH%]	Form of trehalose			Degree of crystallinity (%)		
	40 °C	60 °C	70 °C	40 °C	60 °C	70 °C
0, 0	A	A	A	0	0	0
60, 10	A	A	A	0	0	0
120, 20	A	A	A	0	0	0
180, 30	A	A	h-form	0	0	11.7
240, 40	A	A	h-form	0	0	31.1
300, 45	h-form	h-form	h-form	14.8	27.2	65.2
360, 50	h-form	h-form	h-form	35.8	62.4	100
420, 60	h-form	h-form	$\beta$ /h-form	70.2	78.8	100
480, 70	h-form	h-form	$\beta$ /h-form	100	100	100

The Avrami parameters were obtained from the experimental data by using the double logarithmic form of Eq. (1):

$$\ln[-\ln(1-\alpha)] = \ln K + n \ln t \quad (3)$$

The activation energy of the recrystallization was calculated by using the Arrhenius equation (Eq. (4)):

$$k = k_0 \exp\left(-\frac{E_a}{RT}\right) \quad (4)$$

In the model,  $k$  is the rate constant at temperature  $T$ ,  $k_0$  is the frequency factor,  $R$  is the gas constant and  $E_a$  is the activation energy. The logarithmic form of Eq. (4) allows determination of the activation

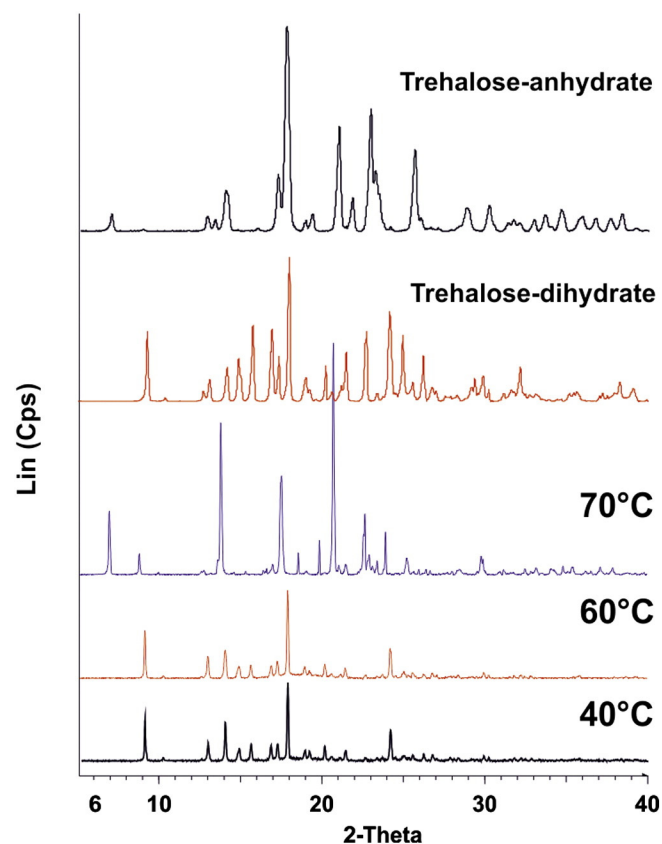


**Fig. 2.** The recrystallized trehalose polymorphs at 40, 60 and 70 °C controlled temperatures.

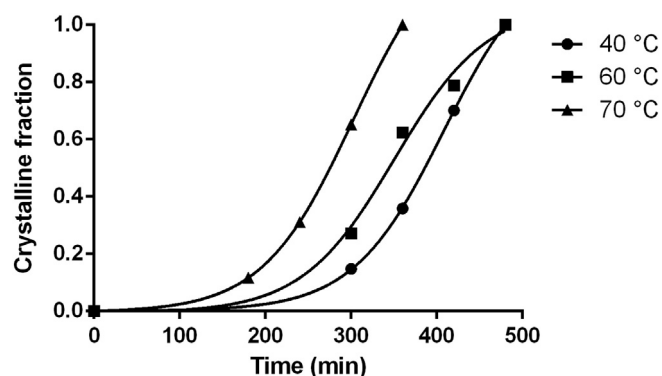


Fig. 3. Crystallization kinetics by fitting the Avrami equation to the HH-XRPD data.

energy (Eq. (5)) (Mazzobre et al., 2001):

$$\ln k = \ln k_0 - \frac{E_a}{RT} \quad (5)$$

## 2.8. DSC

DSC measurements were carried out with a Mettler-Toledo 821<sup>e</sup> DSC instrument (Mettler-Toledo GmbH, Switzerland). Samples loaded at different RH (10, 20, 30, 40, 45, 50 and 70%) in the XRPD humidity chamber for 1 h were crimped in aluminium pans with three holes and were examined in the temperature interval 25–250 °C at a heating rate of 10 °C min<sup>−1</sup> under a constant argon flow of 150 ml min<sup>−1</sup>. Every measurement was normalized to sample size. The fraction of recrystallized trehalose dihydrate was calculated from the integral of sharp endotherm at 108 °C.

## 3. Results and discussion

### 3.1. Determination of calibration curves with XRPD

The peak intensities of the individual components are proportional to the quantities of components in the mixture. Three characteristic peaks each were selected from the diffractograms of trehalose dihydrate (at 8.531°, 12.552° and 14.224° 2θ) and anhydrous trehalose (at 6.572°, 20.351° and 24.792° 2θ). Multiple linear regression (MLR) was used to determine the calibration curve. The dependent variable was the crystallinity and the independent variables were the relative intensity values at chosen 2θ values. After determination of the degree of crystallinity from w/w ratio of the physical mixtures, a calibration curve was fitted. Linear regression of the data produced an  $r^2 = 0.995$  and a slope of 0.990 for trehalose dihydrate (Fig. 1A). For anhydrous trehalose,  $r^2 = 0.997$  and the slope was 0.997 (Fig. 1B).

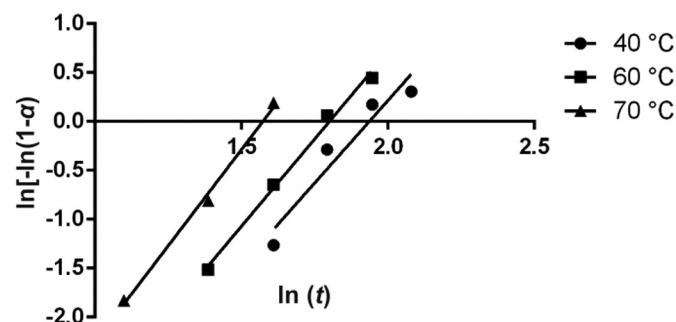


Fig. 4. Determination of the Avrami parameters  $n$  and  $K$  from HH-XRPD data.

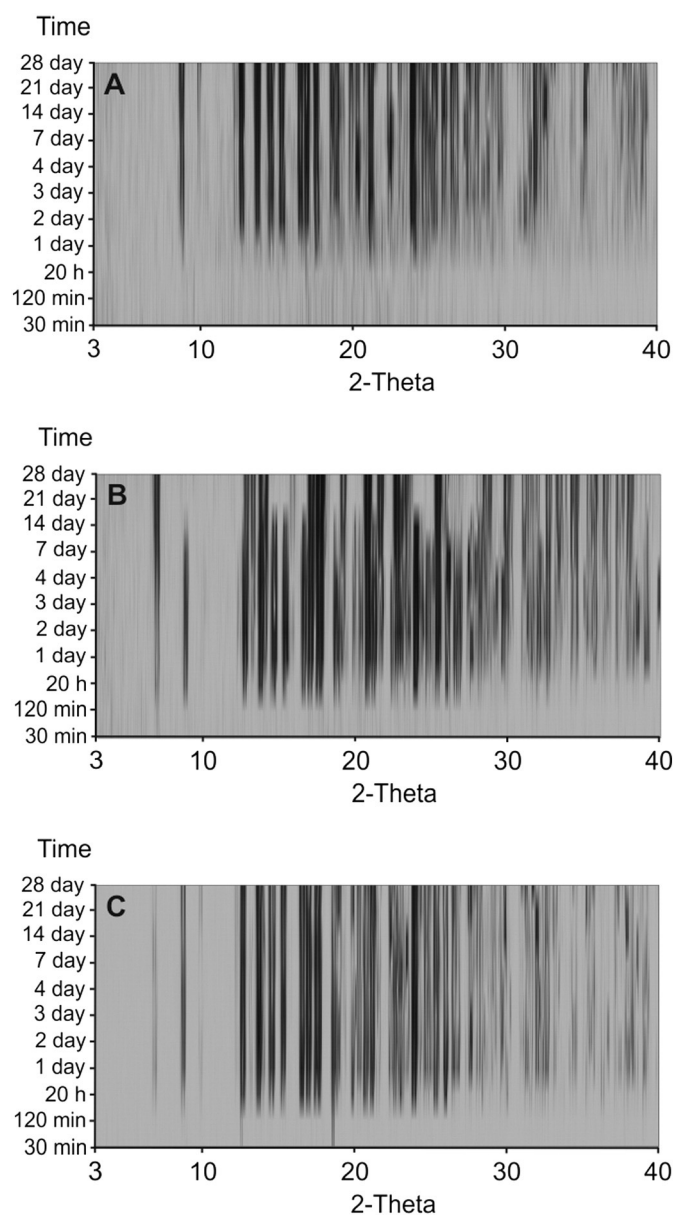


Fig. 5. Top-view pictures of XRPD investigations of samples stored for 28 days at 40 °C, 50% RH (A), 60 °C, 40% RH (B) and 60 °C, 50% RH (C).

Because of the well-correlating  $r^2$  values the degree of crystallinity can be quantified.

### 3.2. Calculation of crystallization kinetics

#### 3.2.1. Hot-humidity stage XRPD analysis

For the development and qualification of solid compositions it is important to investigate and determine changes of the crystalline phases or the effect of crystallization inhibitor, when materials are exposed to changing humidity and temperature. Increasing the humidity in small intervals (10%) at the exact temperature, good estimation could be gained during few hours at the exact temperature about the samples behaviour, which could be reflected on the results of conventional stability test. There is no need for additional hygrometers and extra samples, the measurement takes place directly in the chamber conducted to the instrument. These investigations are not only important to establish procedures for storage, production and shipment, but also emulate the indigestion of the respective drug and its first interactions with the



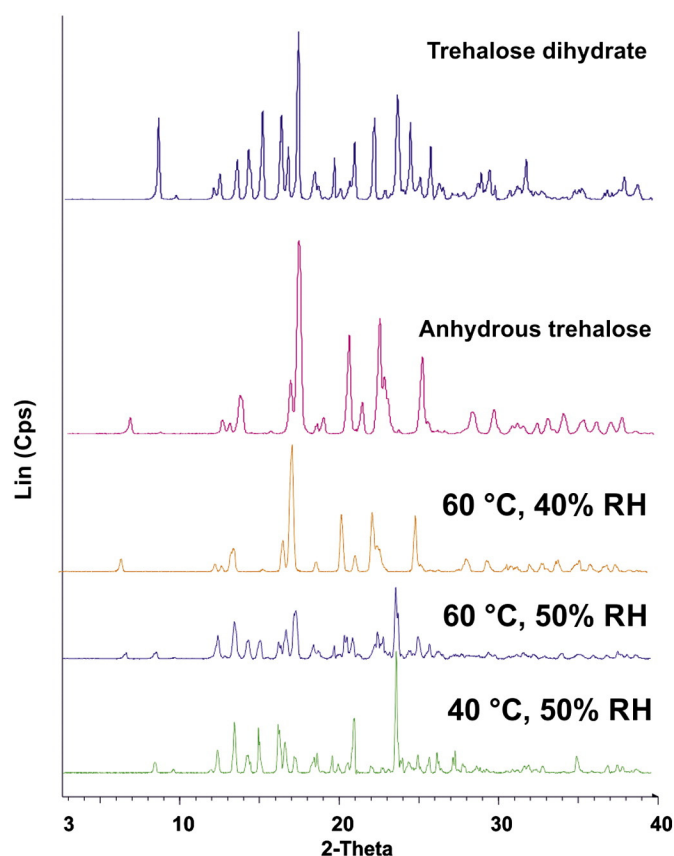


**Fig. 6.** Diffractograms of samples stored for 28 days under different conditions, compared with trehalose forms in CCDC.

patient. In this context HH-XRPD was used to predict the tendency to recrystallization, which is presented in Table 4.

The samples measured at 40 and 60 °C were amorphous up to 45% RH, when recrystallization began in the trehalose dihydrate polymorph. The samples measured at 70 °C were amorphous up to 30% RH, than they recrystallized to dihydrate form and up to 60% RH the anhydrous form appeared too. The determination of the polymorph forms was based on the Cambridge Crystallographic Data Centre (CCDC ID: Al631510) X-ray powder diffractograms (Fig. 2).

The diffractograms measured at 40, 60 and 70 °C showed an increasing tendency to recrystallization. The relative intensities and integrals of the peaks increased with the temperature, and the temperature therefore influences the tendency of trehalose to recrystallize.

To investigate the temperature dependence of recrystallization, the recrystallized fractions were plotted against time for each temperature. As the calibration showed, before XRPD the method could be used for quantitative measurements. The curves obtained by fitting the Avrami

**Table 6**

$\Delta H$  of melting and the crystalline fraction ( $\alpha$ ) at different temperatures with increasing the RH.

RH (%)	$\Delta H$ (J g <sup>-1</sup> )			$\alpha$ (%)		
	40 °C	60 °C	70 °C	40 °C	60 °C	70 °C
30	–	–	17.1	0	0	11
40	–	–	27.3	0	0	17.6
45	44.5	33.0	128.1	28.7	21.3	82.7
50	63.8	66.0	137.6	41.2	42.6	88.8
60	130.4	123.5	141.4	84.2	79.7	91.3
70	153.5	153.0	153.8	99.1	98.8	99.3

Eq. (1) were in good agreement ( $r^2 > 0.992$ ) with the experimental points (Fig. 3).

The sigmoidal curves showed that increased temperature accelerates the recrystallization and reduces the crystallization half-time. To acquire information about the velocity of the process and the dimensions of crystal growth, the parameters  $K$  and  $n$  were determined by using the linearized Avrami equation (Eq. (3)) (Fig. 4) and the activation energy was calculated via the logarithmic form of the Arrhenius model (Eq. (5)) (Table 7).

### 3.2.2. Analysis of samples stored in hygrostats (XRPD)

To the comparison study amorphous samples were stored for 28 days at 40 °C and 60 °C in 3 hygrostats each, where the RH had been set to 30%, 40% and 50%. The fractions of recrystallized trehalose were measured at different times during the 28 days of storage. The conventional XRPD analysis showed, that the samples stored at 40 °C, 30% and 40% RH, and at 60 °C, 30% RH remained amorphous. The samples stored at 40 °C, 50% RH recrystallized in the dihydrate form. The storage conditions at 60 °C, 40% RH, resulted in recrystallization of the anhydrous form, and in the sample stored at 60 °C, 50% RH, both polymorphs appeared, the h-form (dihydrate) and the  $\beta$ -form (anhydrous) (Fig. 5).

Fig. 5B shows that the stripe at 8.531° 2 $\theta$  disappears after storage for 14 days, and there is a polymorph conversion of trehalose dihydrate into the anhydrous form, confirmed by the characteristic thick stripe at 6.572° 2 $\theta$ . Fig. 5A and C do not indicate any polymorph conversion. The diffractograms measured after 28 days storage are shown in Fig. 6.

The degree of crystallinity of the recrystallized polymorphs was calculated by evaluating the diffractograms in Fig. 6 according to the MLR model. The results showed that amorphous fractions remained in the samples, but decreased at higher temperature and RH (Table 5).

By means of the 28-days stability tests, the different recrystallized polymorph forms can be detected and quantified. The results showed that, at 40 °C and 50% RH the dihydrate was detected, but the bulk of the investigated sample remained amorphous. Storage at 60 °C and 40% RH resulted in the appearance of the anhydrous form and only a minor proportion of the sample remained amorphous. At 60 °C and 50% RH, both polymorphic forms were detected and almost the whole sample recrystallized. This conventional method is often used as a long-term stability test in the development of a drug delivery system.

**Table 5**

The degree of crystallinity calculated from the XRPD data after 28 days.

Condition [°C, RH%]	Form of trehalose			Quantity (%)		
	Amorphous	Dihydrate (h-form)	Anhydrous ( $\beta$ -form)	Amorphous	Dihydrate (h-form)	Anhydrous ( $\beta$ -form)
40, 30	+	–	–	100	0	0
40, 40	+	–	–	100	0	0
40, 50	+	+	–	63.1	36.9	0
60, 30	+	–	–	100	0	0
60, 40	+	–	+	25.5	0	74.5
60, 50	+	+	+	0.4	58.2	41.5

**Table 7**

Avrami parameters and activation energy of recrystallization investigated with HH-XRPD and DSC.

Method	$t$ (°C)	$n$	$K$	$E_a$ (kJ mol <sup>-1</sup> )
HH-XRPD	40	3.373	5.79E-04	47.215
	60	3.566	1.70E-03	
	70	3.934	2.84E-03	
DSC	40	3.378	1.69E-03	41.645
	60	2.989	5.98E-03	
	70	3.156	6.29E-03	

### 3.2.3. DSC investigation

The amount of recrystallized trehalose dihydrate was calculated from the integral of the endothermic peaks at 108 °C, which is the melting point of trehalose dehydrate  $\beta$ -form. Table 6 shows the enthalpy changes ( $\Delta H$ ) of melting and the calculated crystalline fraction ( $\alpha$ ) at different temperature increasing the RH.

The amount of crystalline fractions showed, that the recrystallization of the amorphous sample is more significant with increasing RH and at 70% RH total recrystallization of the samples occurred at all 3 temperatures. Comparison of these results with those in Table 4 shows that DSC and HH-XRPD measurements correlate well. With this method, only the fraction of recrystallized trehalose dihydrate can be determined. Since the anhydrous form has high melting point, the dihydrate form is converted into the anhydrous form resulting in false measurement data. However, the method can be used for fast stability testing during the preformulation.

The crystalline fractions calculated from the DSC data (Table 6) were plotted against time for each temperature with  $r^2 > 0.983$  (Fig. 7).

The sigmoidal curves showed that increased temperature accelerates the recrystallization, and reduces the crystallization half-time. To acquire information about the velocity of the process and the dimensions of crystal growth, the Avrami parameters should be determined. The parameters  $K$  and  $n$  were determined by using the linearized Avrami equation (Eq. (3)). A plot of  $\ln[-\ln(1-\alpha)]$  against  $\ln(t)$  yields a straight line with slope  $n$  and intercept  $\ln K$  (Fig. 8). The activation energy was calculated via the logarithmic form of the Arrhenius model (Eq. (5)). Table 6 shows the parameters of the recrystallization process.

The values of rate constant  $K$  show that increasing temperature accelerates the recrystallization process. There are differences between the measurement results of the two methods, but the results correlate well. Comparison of the HH-XRPD data with the DSC measurements demonstrates that increasing temperature accelerates the recrystallization and reduces the crystallization half-time. The parameters  $K$  and  $n$  were determined by using the linearized Avrami equation (Eq. (3)) (Fig. 8).

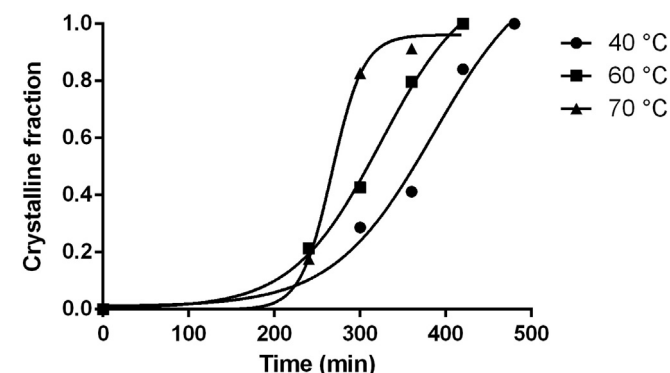


Fig. 7. Crystallization kinetics by fitting the Avrami equation to the DSC data.

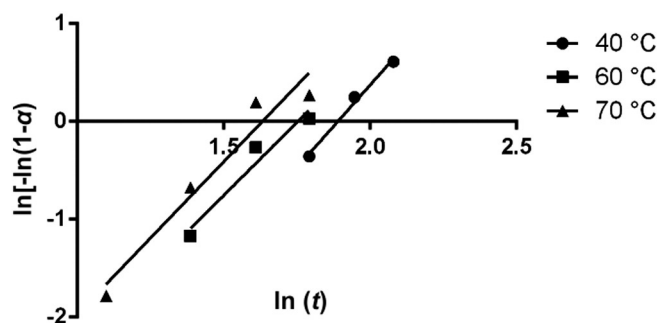


Fig. 8. Determination of Avrami parameters  $n$  and  $K$  from DSC data.

## 4. Conclusions

In the comparison study the three analytical methods (HH-XRPD, XRPD, DSC) were used to investigate the recrystallization of amorphous trehalose. The focus of this work was to suggest such method, which is sensitive and rapid to predict the recrystallization process in the preformulation study.

HH-XRPD was used to investigate the effects of temperature and rapid RH changes. Different RH conditions resulted in different crystalline forms of trehalose, which means that recrystallization can start during the process of the investigation. In this way, the control of crystallinity is necessary. The measurement demonstrated that the recrystallization began at 40 and 60 °C up to 45% RH and at 70 °C up to 30% RH into dihydrate form. At 70 °C up to 60% RH, the anhydrous form of trehalose appeared too. It could be concluded that the temperature and RH dependence of recrystallization are determining factors. This can be expressed in a numerical relationship by the Avrami and Arrhenius equations. HH-XRPD is a good choice for gaining a good estimation over a few hours about the samples behaviour, which could be reflected on the results of a conventional stability test.

The conventional storage at different temperatures and RH gave information about the recrystallized polymorphs. Over the course of 28 days, both RH and temperature changes can cause the recrystallization of amorphous trehalose. The dihydrate form was detected at 40 °C, 50% RH. Storage at 60 °C, 40% RH resulted in the appearance of the anhydrous form and at 60 °C, 50% RH both polymorphic forms were detected. In this light, the suitable choice of the storage conditions can protect the amorphous trehalose samples from crystallization.

By carrying out the DSC measurements at different temperatures, the fraction of recrystallized trehalose dihydrate can be determined. The degree of crystallinity of trehalose dihydrate determined by DSC correlated well with the HH-XRPD measurements.

It could be concluded that HH-XRPD is faster than other conventional techniques and a good prediction for the recrystallization of amorphous compounds during preformulation, moreover the physical changes could be studied on one sample.

## References

- Aguib, Y., Heiseke, A., Gilch, S., Riemer, C., Baier, M., Schatzl, H.M., Ertmer, A., 2009. Autophagy induction by trehalose counteracts cellular prion infection. *Autophagy* 5, 361–369.
- Amaro, M.I., Tajber, L., Corrigan, O.I., Healy, A.M., 2015. Co-spray dried carbohydrate microparticles: crystallization delay/inhibition and improved aerosolization characteristics, through the incorporation of hydroxypropyl- $\beta$ -cyclodextrin with amorphous raffinose or trehalose. *Pharm. Res.* 32, 180–195.
- Claus, S., Schoenbrodt, T., Weiler, C., Friess, W., 2011. Novel dry powder inhalation system based on dispersion of lyophilisates. *Eur. J. Pharm. Sci.* 43, 32–40.
- Crowe, J.H., Tablin, F., Wolters, W.F., Gousset, K., Tsvetkova, N.M., Ricker, J., 2003. Stabilization of membranes in human platelets freeze-dried with trehalose. *Chem. Phys. Lipids* 122, 41–52.
- Danciu, C., Soica, C., Oltean, M., Avram, S., Borcan, F., Csányi, E., Ambrus, R., Zupkó, I., Muntean, D., Dehelean, C.A., Craina, M., Popovici, R.A., 2014. Genistein in 1:1 inclusion complexes with ramified cyclodextrins: theoretical, physicochemical and biological evaluation. *Int. J. Mol. Sci.* 15, 1962–1982.

- Furuki, T., Kishi, A., Sakurai, M., 2005. De- and rehydration behavior of  $\alpha,\alpha$ -trehalose dihydrate under humidity-controlled atmospheres. *Carbohydr. Res.* 340, 429–438.
- Gradon, L., Sosnowski, T.R., 2014. Formation of particles for dry powder inhalers. *Adv. Powder Technol.* 25, 43–55.
- Guguta, C., Meekes, H., de Gelder, R., 2008. The hydration/dehydration behavior of aspartame revisited. *J. Pharm. Biomed. Anal.* 46, 617–624.
- Guguta, C., van Eck, E.R.H., de Gelder, R., 2009. Structural insight into the dehydration and hydration behavior of naltrexone and naloxone hydrochloride. *Dehydration-induced expansion versus contraction. Cryst. Growth Des.* 9, 3384–3395.
- Islam, N., Gladki, E., 2008. Dry powder inhalers (DPIs)—a review of device reliability and innovation. *Int. J. Pharm.* 360, 1–11.
- Jójárt-Laczkovich, O., Szabó-Révész, P., 2010. Amorphization of a crystalline active pharmaceutical ingredient and thermoanalytical measurements on this glassy form. *J. Therm. Anal. Cal.* 102, 243–247.
- Jójárt-Laczkovich, O., Szabó-Révész, P., 2011. Formulation of tablets containing an 'inprocess' amorphized active pharmaceutical ingredient. *Drug Dev. Ind. Pharm.* 37, 1272–1281.
- Jones, M.D., Hooton, J.C., Dawson, M.L., Ferrie, A.R., Price, R., 2006. Dehydration of trehalose dihydrate at low relative humidity and ambient temperature. *Int. J. Pharm.* 313, 87–98.
- Jovanovic, N., Bouchard, A., Hofland, G.W., Witkamp, G.J., Crommelin, D.J.A., Jiskoot, W., 2006. Distinct effects of sucrose and trehalose on protein stability during supercritical fluid drying and freeze-drying. *Eur. J. Pharm. Sci.* 27, 336–345.
- Jug, M., Bećirević-Lačan, M., 2004. Influence of hydroxypropyl- $\beta$ -cyclodextrin complexation on piroxicam release from buccoadhesive tablets. *Eur. J. Pharm. Sci.* 21, 251–260.
- Kara, N.Z., Tokar, L., Agam, G., Anderson, G.W., Belmaker, R.H., Einat, H., 2013. Trehalose induced antidepressant-like effects and autophagy enhancement in mice. *Psychopharmacology* 229, 367–375.
- Maas, S.G., Schaldach, G., Littringer, E.M., Mescher, A., Griesser, U.J., Braun, D.E., Walzel, P.E., Urbanetz, N.A., 2011. The impact of spray drying outlet temperature on the particle morphology of mannitol. *Powder Technol.* 213, 27–35.
- Mah, P.T., Laaksonen, T., Rades, T., Peltonen, L., Strachan, C.J., 2015. Differential scanning calorimetry predicts the critical quality attributes of amorphous glibenclamide. *Eur. J. Pharm. Sci.* 80, 74–81.
- Maurya, M., Murphy, K., Kumar, S., Shib, L., Lee, G., 2005a. Effects of process variables on the powder yield of spray-dried trehalose on a laboratory spray-dryer. *Eur. J. Pharm. Biopharm.* 59, 565–573.
- Maurya, M., Murphy, K., Kumar, S., Mauerer, A., Lee, G., 2005b. Spray-drying of proteins: effects of sorbitol and trehalose on aggregation and FT-IR amide I spectrum of an immunoglobulin G. *Eur. J. Pharm. Biopharm.* 59, 251–261.
- Mazzobre, M.F., Soto, G., Aguilera, J.M., Buera, M.P., 2001. Crystallization kinetics of lactose in systems co-lyophilized with trehalose. *Analysis by differential scanning calorimetry. Food Res. Int.* 34, 903–911.
- Moran, A., Buckton, G., 2007a. Adjusting and understanding the properties and crystallisation behaviour of amorphous trehalose as a function of spray drying feed concentration. *Int. J. Pharm.* 343, 12–17.
- Moran, A., Buckton, G., 2007b. Adjusting and understanding the properties and crystallisation behaviour of amorphous trehalose as a function of spray drying feed concentration. *Int. J. Pharm.* 343, 12–17.
- Murugappan, S., Patil, H.P., Kanojia, G., ter Veer, W., Meijerhof, T., Frijlink, H.W., Huckriede, A., Hinrichs, W.L.J., 2013. Physical and immunogenic stability of spray freeze-dried influenza vaccine powder for pulmonary delivery: comparison of inulin, dextran, or a mixture of dextran and trehalose as protectants. *Eur. J. Pharm. Biopharm.* 85, 716–725.
- Nagase, H., Endo, T., Ueda, H., Nakagaki, M., 2002. An anhydrous polymorphic form of trehalose. *Carbohydr. Res.* 337, 167–173.
- Nakamura, T., Sekiyama, E., Takaoka, M., Bentley, A.J., Yokoi, N., Fullwood, N.J., Kinoshita, S., 2008. The use of trehalose-treated freeze-dried amniotic membrane for ocular surface reconstruction. *Biomaterials* 29, 3729–3737.
- Ógáin, O.N., Li, J., Tajber, L., Corrigan, O.I., Healy, A.M., 2011. Particle engineering of materials for oral inhalation by dry powder inhalers. I-particles of sugar excipients (trehalose and raffinose) for protein delivery. *Int. J. Pharm.* 405, 23–35.
- Pomázi, A., Ambrus, R., Sipos, P., Szabó-Révész, P., 2011. Analysis of co-spray-dried meloxicam-mannitol systems containing crystalline microcomposites. *J. Pharm. Biomed. Anal.* 56, 183–190.
- Sussich, F., Cesáro, A., 2008. Trehalose amorphization and recrystallization. *Carbohydr. Res.* 343, 2667–2674.
- Szakonyi, G., Zelkó, R., 2012. The effect of water on the solid state characteristics of pharmaceutical excipients: molecular mechanisms, measurement techniques, and quality aspects of final dosage form. *Int. J. Pharm. Investig.* 2, 18–25.
- Tanaka, K., Takeda, T., Fujii, K., Miyajima, K., 1992. Cryoprotective mechanism of saccharides on freeze-drying of liposome. *Chem. Pharm. Bull.* 40, 1–5.
- Taylor, L.S., York, P., 1998. Effect of particle size and temperature on the dehydration kinetics of trehalose dihydrate. *Int. J. Pharm.* 167, 215–221.
- Timasheff, S.N., 2002. Protein hydration, thermodynamic binding, and preferential hydration. *Biochemistry* 41, 13473–13482.
- Tonnies, W.F., Amorij, J.P., Vreeman, M.A., Frijlink, H.W., Kersten, G.F., Hinrichs, W.L.J., 2014. Improved storage stability and immunogenicity of hepatitis B vaccine after spray-freeze drying in presence of sugars. *Eur. J. Pharm. Sci.* 55, 36–45.
- Yu, Z., Johnston, K.P., Williams, R.O., 2006. Spray freezing into liquid versus spray-freeze drying: influence of atomization on protein aggregation and biological activity. *Eur. J. Pharm. Sci.* 27, 9–18.